

Phase diagram of the ionic Hubbard model with density-dependent hopping

P. Roura-Bas

Centro Atómico Bariloche, GAIDI, CONICET, 8400 Bariloche, Argentina

A. A. Aligia

*Instituto de Nanociencia y Nanotecnología CNEA-CONICET, GAIDI,
Centro Atómico Bariloche and Instituto Balseiro, 8400 Bariloche, Argentina*

We obtain the quantum phase diagram of the ionic Hubbard model including electron-hole symmetric density-dependent hopping. The boundaries of the phases are determined by crossing of excited levels with particular discrete symmetries, which coincide with jumps of charge and spin Berry phases with a topological meaning. Reducing the magnitude of the hopping terms that do not change the total number of singly occupied sites with respect to the other one, the region of the phase diagram occupied by the fully gapped spontaneously dimerized insulator (which separates the band insulating and Mott insulating phases) is enlarged, particularly for small values of the alternating on-site energy. This result might be relevant for experiments in cold atoms in which topological charge pumping is observed when alternation in the hopping is included.

I. INTRODUCTION

Ultracold quantum gases provide a versatile platform as universal quantum simulators of many-body problems¹. Cold atoms as well as other platforms have been used to study quantized topological charge pumping in driven systems². A time dependent adiabatic evolution in a closed cycle in a certain space of parameters constitute a Thouless pump, in which a quantized amount of charge or spin is transported, which is topologically protected^{3,4}. Simulating the non-interacting Rice-Mele model (RMM)⁵ with ultracold atoms, quantized charge pumping has been achieved for bosons⁶ and fermions⁷. More recently, charge pumping in the fermionic interacting RMM (IRMM) has been studied experimentally⁸ and theoretically^{9,10}, including spin pumping¹⁰.

The IRMM is a one-dimensional Hubbard model which includes alternating on-site energies $\pm\Delta$ and hopping $t\pm\delta$ [Eq. (1) with $t_{\alpha\beta} = t$]. Ideally, in a Thouless pump, a critical point of degeneracy is surrounded in the adiabatic time cycle without closing a gap. For the IRMM, and fixed on-site interaction U , the cycles which lead to non-trivial charge pumping enclose critical points lying at $\delta = 0$ and $\Delta = \pm\Delta_c$. For $\delta = 0$, the IRMM is equivalent to the ionic Hubbard model (IHM)^{11–16} and it is known that at $\Delta = \pm\Delta_c$ there is a charge transition in which the topologically protected charge Berry phase jumps between the values 0 and π ¹², implying a transport of one charge when a time cycle is performed in the plane (δ, Δ) enclosing the point $(0, \pm\Delta_c)$ ^{10,17}.

Similarly at $\Delta = \pm\Delta_s$ there is a spin transition in the IHM ($\delta = 0$) with a jump in the spin Berry phase and a closing of the spin gap for $|\Delta| \leq \Delta_s < \Delta_c$. The IHM has three phases. The system is a Mott insulator (MI) for $0 \leq \Delta < \Delta_s$, a band insulator (BI) for $\Delta > \Delta_c$ and a spontaneously dimerized insulator (SDI) in a narrow region between the other two. The phase diagram (which is symmetric by a change of sign in Δ) has been constructed in Ref. 12 using the method of crossing of

excited energy levels (MCEL) based on conformal field theory^{21–25}. The spin gap opens as $|\delta|^{2/3}$ leading to a dimerized phase for finite δ ¹⁰.

The fact that the spin gap vanishes in the MI phase (that corresponds to $\delta = 0$, $-\Delta_s < \Delta < \Delta_s$) brings problems for the charge pumping. A cycle in the plane δ, Δ that encloses a critical point $\Delta = \pm\Delta_c$ and passes far from it, necessarily traverses the MI phase, because Δ_c and Δ_s are very near each other. Traversing with a finite velocity a gapless point produces spin excitation at finite energy, which in turn lead to charge excitations because of the mixing of both sectors at finite energy^{11,14}. This leads to oscillations in the charge pumping and loss of quantization with the number of cycles as determined theoretically¹⁰ and experimentally²⁶. While addition of a staggered magnetic field or Ising spin interactions lead to opening of the spin gap and robust charge pumping¹⁰, these terms are not experimentally feasible at present.

Another possibility to enlarge the spin gap and the region of stability of the SDI phase is to add a density-dependent hopping (DDH). Such a term in an electron-hole symmetric form has been realized in cold atoms using Floquet engineering^{27–32}. The Hubbard model with nearest-neighbor hopping dependent on the occupancy of the sites involved (also called correlated hopping) has been derived and studied as an effective model for the superconducting cuprates^{33–35}, which leads to enhancement of superconductivity for certain parameters^{36–39}. In one dimension, it has been found that when the hopping term that changes the number of singly occupied sites [t_{AB} in Eq. (1)] is larger than the other two, a dimerized phase with a spin gap is favored^{18–21}, which is the desired effect.

The goal of this work is to study to what extent the region of the phase diagram of the IHM occupied by the fully gapped SDI phase can be enlarged including DDH. We use the method of crossing of excited energy levels (MCEL) based on conformal field theory^{21–25}, already used in Ref. 12 for the standard IHM. For this model including DDH, the method also coincides with that of

jumps of charge and spin Berry phases used in Ref. 20.

The paper is organized as follows. In Section II we explain the model and methods. The resulting phase diagram is contained in Section III. Section IV contains a summary and discussion.

II. MODEL AND METHODS

The IRMM including DDH has the form

$$\begin{aligned}
 H = & \sum_{j\sigma} [-1 + \delta (-1)^j] \left(c_{j\sigma}^\dagger c_{j+1\sigma} + \text{H.c.} \right) \\
 & \times [t_{AA}(1 - n_{j\bar{\sigma}})(1 - n_{j+1\bar{\sigma}}) + t_{BB}n_{j\bar{\sigma}}n_{j+1\bar{\sigma}} \\
 & + t_{AB}(n_{j\bar{\sigma}} + n_{j+1\bar{\sigma}} - 2n_{j\bar{\sigma}}n_{j+1\bar{\sigma}})] \\
 & + \Delta \sum_{j\sigma} (-1)^j n_{j\sigma} + U \sum_j n_{j\uparrow} n_{j\downarrow}. \quad (1)
 \end{aligned}$$

The first term is the DDH, which is alternating for $\delta \neq 0$. The amplitude t_{AA} corresponds to the situation in which only the particle that hops occupies the two nearest-neighbor sites involved in the hopping. For t_{AB} and t_{BB} the total occupancy is 2 and 3 respectively. In the following we assume the electron-hole symmetric case $t_{BB} = t_{AA}$, which is the one implemented experimentally with cold atoms²⁷⁻³². Δ is the alternating on-site energy and U is the on-site Coulomb repulsion, both characteristic of the IHM¹¹⁻¹⁶.

Our conclusions, and our discussions below on the effect of the alternation of the hopping δ are the same if δ affects only the hopping part proportional to t_{AB} , and not the other two.

In experiment usually the pump cycles are done in a two-dimensional space (δ, p) in which both δ and another parameter p (like Δ or U) depend on time and return to the original value after the cycle. In the adiabatic limit, the charge (spin) pumped in the cycle is determined by the evolution of the charge (spin) Berry phase γ_c (γ_s) in the cycle (see for example Ref. 10). Non trivial quantized charge (spin) pumping takes place when a critical point at which γ_c (γ_s) jumps, is surrounded in the cycle. The critical points lie on the line $\delta = 0$, because for $\delta = 0$, the system has inversion symmetry at each site and as a consequence, the Berry phases can only be either 0 or π (mod 2π). In other words, γ_c/π and γ_s/π become topological numbers protected by inversion symmetry¹⁷. In addition, the MI phase in which the spin gap vanishes is also restricted to $\delta = 0$. Then to identify a possible cycle that encloses the charge critical point with a ground state separated from the rest of the spectrum in the whole cycle, one can keep $\delta = 0$, where all ground-state degeneracies lie. This is what we do in the rest of the work. The model becomes the IHM with electron-hole symmetric DDH.

To calculate the phase diagram of the model we use the MCEL²¹⁻²⁵. The idea of the method is that the dominant correlations at large distances correspond to the smallest

excitation energies. The crossing of excited levels in different symmetry sectors therefore correspond to phase transitions. The method has been used before for similar models^{12,20,21}. For our model, this method and the jumps in the values of the Berry phases give the same information¹², but the MCEL is easier to implement.

The crossing for both charge and spin transitions are determined using open-shell boundary conditions (periodic if the number of sites L is multiple of 4, antiperiodic for L even not multiple of 4). The charge transition is determined by a crossing in the ground state of the two singlets of lowest energy with opposite parity under inversion. In the BI phase the ground state is even under inversion, while it is odd in the other two phases. The spin transition between SDI and MI phases, is determined by the crossing of the excited even singlet with lowest energy and the lowest excited odd triplet, which has less energy in the MI phase. In the actual calculation we have not evaluated the total spin S of the states, but used the parity under time reversal (the singlet is even and the triplet with total spin projection $S_z = 0$ is odd). All these states have wave vector 0 for $\Delta \neq 0$.

To determine the phase diagram we have set $t_{AB} = 1$ as the unit of energy. Then for a given value of t_{AA} and Δ we have calculated the values of U that correspond to the charge (U_c) and spin (U_s) transitions using the MCEL for all even number of sites L in the range $6 \leq L \leq 14$. The results were extrapolated to $L \rightarrow \infty$ using a quadratic polynomial in $1/L$. Examples of the extrapolation are shown in Fig. 1. The curves fits well the data and the finite-size effects are in general small, except for the charge transition for small values of Δ . In any case, a deviation of the value of U_c for $\Delta = 0.2$ for up to 20% is very unlikely from the trend of the curve and does not modify our conclusions.

III. RESULTS

In Fig. 2, we compare the phase diagram of the standard IHM with that in which the hopping terms that do not alter the total number of singly occupied sites $t_{AA} = t_{BB}$ is reduced. For fixed Δ the system is a BI for low U and a MI for large U . Both phases are separated by a narrow region of the SDI phase. Increasing U , the charge transition at $U = U_c$ (with a jump in γ_c from 0 to π^{12}) corresponds to the change from the BI to the SDI, and at the spin transition for $U = U_s$ (with a jump in γ_c from 0 to π^{12}) the SDI changes to the MI.

For $\Delta > \sim 3t_{AB}$ the width of the SDI phase is of the order of a fraction of t_{AB} . Naturally, keeping the three hopping terms equal $t_{\alpha\beta} = t$ and reducing t the SDI phase shrinks and both $U_c, U_s \rightarrow 2\Delta$ for $t \rightarrow 0$. It is therefore noticeable that reducing only $t_{AA} = t_{BB}$, the extension of the SDI phase is *increased* and by about 20% for $\Delta > 3t_{AB}$.

As it is apparent in Fig. 3, this effect is more dramatic for $\Delta < 0.5t_{AB}$. In fact, contrary to the case of equal

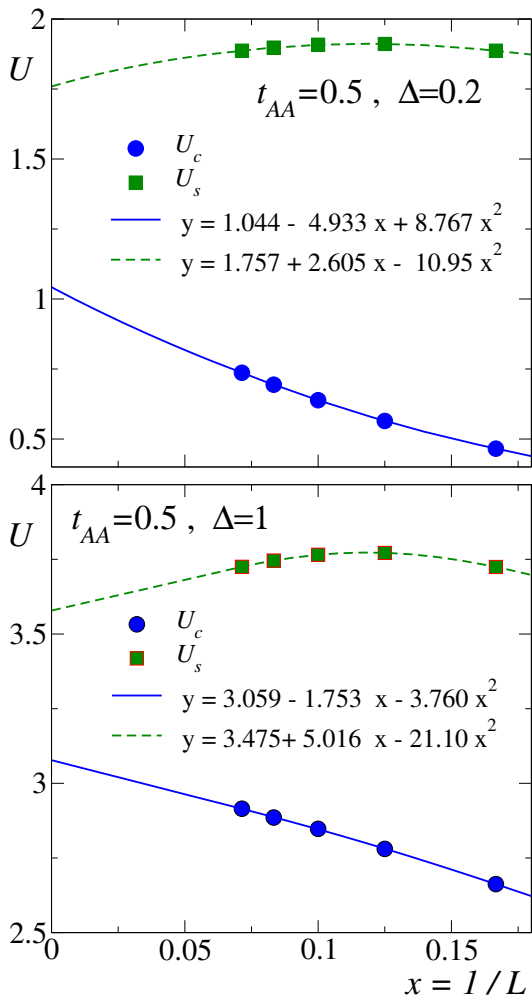


FIG. 1. (Color online) Critical values of U for the charge and spin transitions for $t_{AB} = 1$, and other parameters indicated inside each figure.

$t_{\alpha\beta} = t$, there is a finite spin gap for small U even at $\Delta = 0$ when $t_{AB} > t_{AA} = t_{BB}$. This result has been found before¹⁸⁻²¹ and can be understood from analytical calculations using bosonization^{18,19} which coincide very well with numerical calculations²⁰ for small values of U .

The particular features of the phase diagram for small Δ , render it possible to perform time evolutions around a critical point for the charge transition that transport a quantized unit of charge per cycle with open charge and spin gaps in the whole cycle. For example for $\Delta = 0.3$, $t_{AB} = 1$, and $t_{AA} = t_{BB} = 0.5$, we find $U_c = 0.91$ and $U_s = 2.14$. Similarly for $\Delta = 0.4$ we find $U_c = 1.22$ and $U_s = 2.38$. Performing a time dependent cycle in the plane either (δ, Δ) or (δ, U) with center at the charge critical point (with $\delta = 0$) and amplitude in Δ of about ± 0.25 or in U near ± 0.5 , the cycle never reaches the MI phase and therefore, the spin gap is always open. One point that should be taken into account is that the spin transition is of the Kosterlitz-Thouless type, and

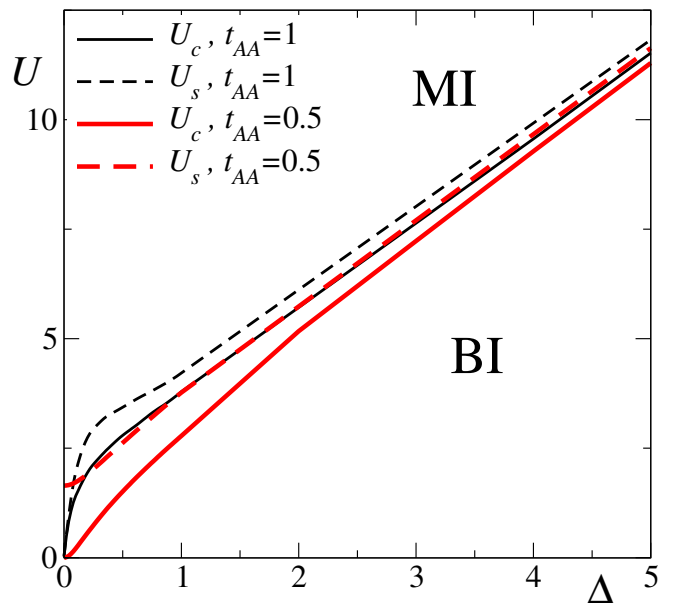


FIG. 2. (Color online) Phase diagram of the IHM with DDH in the Δ, U plane for $t_{AB} = 1$, and two values of $t_{AA} = t_{BB}$. The region between the full and dashes lines corresponds to the SDI.

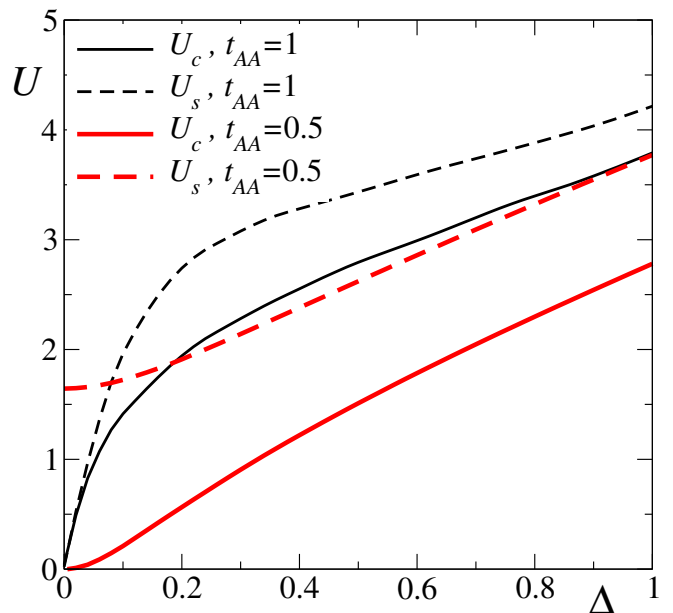


FIG. 3. Same as Fig. 2 in a smaller region of Δ .

therefore the spin gap is exponentially small in the SDI phase near the transition boundary²⁰. Therefore it might be convenient to move the time cycle away from the MI-SDI boundary, keeping the critical point inside it.

In the previous figures we have taken $t_{AA} = t_{BB} = t_{AB}/2$. In Fig. 4 we show how the values of U at both transitions change with $t_{AA} = t_{BB}$ for a small value of Δ .

We can see that the change is more rapid for t_{AA} near t_{AB} and the increase in U_s is already large for $t_{AA}/t_{AB} = 3/4$. Note also that when t_{AA}/t_{AB} exceeds 1 for a significant amount U_c becomes larger than U_s giving rise to a new phase in between. The properties of this phase are beyond the scope of the present work. For $\Delta = 0$, this phase corresponds to a Tomonaga-Luttinger liquid with triplet superconducting and bond spin-density wave correlations dominating at large distances^{18–20}, but Δ is a relevant perturbation that modifies the physics.

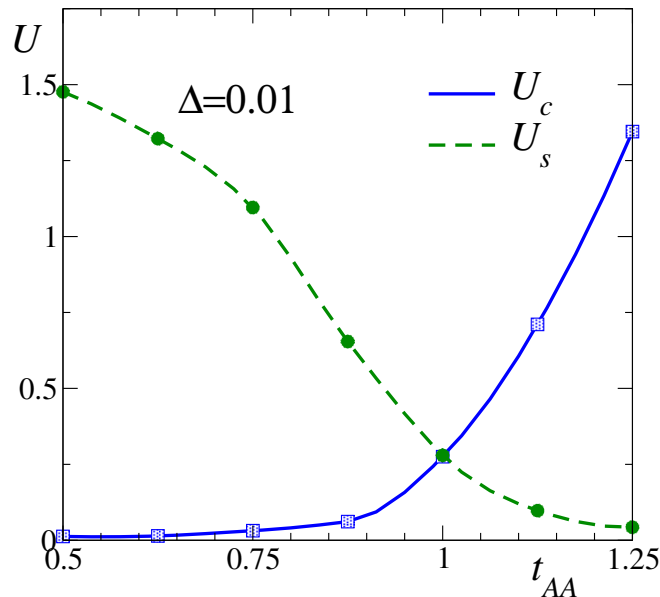


FIG. 4. (Color online) Critical values of U at the charge and spin transitions as a function of $t_{AA} = t_{BB}$ for $t_{AB} = 1$ and $\Delta = 0.01$.

IV. SUMMARY AND DISCUSSION

We have calculated the quantum phase diagram of the IHM including electron-hole symmetric DDH, which corresponds to Eq. (1) with $\delta = 0$ and $t_{AA} = t_{BB} < t_{AB}$, using the MCEL in rings of up to 14 sites. We obtain that a reduction of $t_{AA} = t_{BB}$ with respect to t_{AB} , increases the region of the phase diagram occupied by the fully gapped SDI phase, particularly for $|\Delta| < t_{AB}$ and $U < 2t_{AB}$.

This result is of possible relevance to experiments with cold atoms for which quantized pumping is observed, but crossing the spin gapless MI phase leads to oscillation and the breakdown of topological pumping after the first cycle. Floquet engineering renders it possible to achieve the region $t_{AA} = t_{BB} < t_{AB}$ and enlarge the region of the gapped SDI phase. To confirm the possibilities of this proposal, it would be useful to calculate the spin gap and the internal gap between even and odd singlets in the SDI phase. This would require a study of longer chains using density-matrix renormalization group. It would also be useful to simulate the time dependence in pumping cycles similar to the ones suggested here, using infinite time-evolving block decimation.

ACKNOWLEDGMENTS

We thank Konrad Viebahn, Eric Bertok and Fabian Heidrich-Meisner for useful discussions. AAA acknowledges financial support provided by PICT 2017-2726 and PICT 2018-01546 of the ANPCyT, Argentina.

- ¹ G. Gross and I. Bloch, Quantum simulations with ultracold atoms in optical lattices, *Science* **357**, 995 (2017).
- ² R. Citro and M. Aidelsburger, Thouless pumping and topology, *Nat. Rev. Phys.* **5**, 87 (2023).
- ³ D. J. Thouless, Quantization of particle transport, *Phys. Rev. B* **27**, 6083 (1983).
- ⁴ Q. Niu and D. J. Thouless, Quantised adiabatic charge transport in the presence of substrate disorder and many-body interaction, *J. Phys. A: Math. Gen.* **17**, 2453 (1984).
- ⁵ M. J. Rice and E. J. Mele, Elementary Excitations of a Linearly Conjugated Diatomic Polymer, *Phys. Rev. Lett.* **49**, 1455 (1982).
- ⁶ S. Nakajima, T. Tomita, S. Taie, T. Ichinose, H. Ozawa, L. Wang, M. Troyer, and Y. Takahashi, Topological Thouless pumping of ultracold fermions, *Nat. Phys.* **12**, 296 (2016).
- ⁷ M. Lohse, C. Schweizer, O. Zilberberg, M. Aidelsburger, and I. Bloch, A Thouless quantum pump with ultracold bosonic atoms in an optical superlattice *Nat. Phys.* **12**, 350 (2016).
- ⁸ A.-S. Walter, Z. Zhu, M. Gächter, J. Minguzzi, S. Roschinski, K. Sandholzer, K. Viebahn, and T. Esslinger, Breakdown of quantisation in a Hubbard-Thouless pump

- arXiv:2204.06561.
- ⁹ M. Nakagawa, T. Yoshida, R. Peters, and N. Kawakami, Breakdown of topological Thouless pumping in the strongly interacting regime, *Phys. Rev. B* **98**, 115147 (2018).
- ¹⁰ E. Bertok, F. Heidrich-Meisner, and A. A. Aligia, Splitting of topological charge pumping in an interacting two-component fermionic Rice-Mele Hubbard model, *Phys. Rev. B* **106**, 045141 (2022).
- ¹¹ M. Fabrizio, A.O. Gogolin, and A.A. Nersisyan, From Band Insulator to Mott Insulator in One Dimension, *Phys. Rev. Lett.* **83**, 2014 (1999).
- ¹² M. E. Torio, A. A. Aligia, and H. A. Ceccatto, Phase diagram of the Hubbard chain with two atoms per cell, *Phys. Rev. B* **64**, 121105(R) (2001).
- ¹³ S. R. Manmana, V. Meden, R. M. Noack, and K. Schönhammer, Quantum critical behavior of the one-dimensional ionic Hubbard model, *Phys. Rev. B* **70**, 155115 (2004).
- ¹⁴ A. A. Aligia, Charge dynamics in the Mott insulating phase of the ionic Hubbard model, *Phys. Rev. B* **69**, 041101(R) (2004).

- ¹⁵ M. E. Torio, A. A. Aligia, G. I. Japaridze, and B. Normand, Quantum phase diagram of the generalized ionic Hubbard model for AB_n chains, *Phys. Rev. B* **73**, 115109 (2006).
- ¹⁶ L. Stenzel, A. L. C. Hayward, C. Hubig, U. Schollwöck, and F. Heidrich-Meisner, Quantum phases and topological properties of interacting fermions in one-dimensional superlattices, *Phys. Rev. A* **99**, 053614 (2019).
- ¹⁷ A. A. Aligia, Topological invariants based on generalized position operators and application to the interacting Rice-Mele model, *Phys. Rev. B* **107**, 075153 (2023).
- ¹⁸ G. I. Japaridze and A. P. Kampf, Weak-coupling phase diagram of the extended Hubbard model with correlated-hopping interaction, *Phys. Rev. B* **59**, 12822 (1999).
- ¹⁹ A. A. Aligia and L. Arrachea, Triplet superconductivity in quasi-one-dimensional systems *Phys. Rev. B* **60**, 15332 (1999).
- ²⁰ A. A. Aligia, K. Hallberg, C.D. Batista and G. Ortiz, Phase diagrams from topological transitions: The Hubbard chain with correlated hopping, *Phys. Rev. B* **61**, 7883 (2000).
- ²¹ M. Nakamura, Tricritical behavior in the extended Hubbard chains, *Phys. Rev. B* **61**, 16377 (2000).
- ²² K. Nomura and K. Okamoto, Critical properties of $S=1/2$ antiferromagnetic XXZ chain with next-nearest-neighbour interactions, *J. Phys. A* **27**, 5773 (1994).
- ²³ M. Nakamura, K. Nomura, and A. Kitazawa, Renormalization Group Analysis of the Spin-Gap Phase in the One-Dimensional $t-J$ Model, *Phys. Rev. Lett.* **79**, 3214 (1997).
- ²⁴ M. Nakamura, Mechanism of CDW-SDW Transition in One Dimension, *J. Phys. Soc. Jpn.* **68**, 3123 (1999).
- ²⁵ R. D. Somma and A. A. Aligia, Phase diagram of the XXZ chain with next-nearest-neighbor interactions, *Phys. Rev. B* **64**, 024410 (2001).
- ²⁶ A.-S. Walter *et al.* in preparation
- ²⁷ R. Ma, M. E. Tai, P. M. Preiss, W. S. Bakr, J. Simon, and M. Greiner, Photon-assisted tunneling in a biased strongly correlated Bose gas, *Phys. Rev. Lett.* **107**, 095301 (2011).
- ²⁸ F. Meinert, M. J. Mark, K. Lauber, A. J. Daley, and H.-C. Nägerl, Floquet engineering of correlated tunneling in the Bose-Hubbard model with ultracold atoms, *Phys. Rev. Lett.* **116**, 205301 (2016).
- ²⁹ R. Desbuquois, M. Messer, F. Görg, K. Sandholzer, G. Jotzu, and T. Esslinger, Controlling the Floquet state population and observing micromotion in a periodically driven two-body quantum system, *Phys. Rev. A* **96**, 053602 (2017).
- ³⁰ F. Görg, M. Messer, K. Sandholzer, G. Jotzu, R. Desbuquois, and Tilman Esslinger Enhancement and sign change of magnetic correlations in a driven quantum many-body system *Nature* **553**, 481 (2018).
- ³¹ M. Messer, K. Sandholzer, F. Görg, J. Minguzzi, R. Desbuquois, and T. Esslinger, Floquet Dynamics in Driven Fermi-Hubbard Systems *Phys. Rev. Lett.* **121**, 233603 (2018)
- ³² F. Görg, K. Sandholzer, J. Minguzzi, R. Desbuquois, M. Messer, and T. Esslinger, Realization of density-dependent Peierls phases to engineer quantized gauge fields coupled to ultracold matter, *Nature Physics* **15**, 1161 (2019).
- ³³ H.B. Schüttler and A.J. Fedro, Copper-oxygen charge excitations and the effective-single-band theory of cuprate superconductors, *Phys. Rev. B* **45**, 7588 (1992).
- ³⁴ M. E. Simon, M. Balaña and A. A. Aligia, Effective one-band hamiltonian for cuprate superconductor metal-insulator transition, *Physica C* **206**, 297 (1993).
- ³⁵ M. E. Simon and A. A. Aligia, Brinkman-Rice transition in layered perovskites, *Phys. Rev. B* **48**, 7471 (1993).
- ³⁶ J. Hirsch, Bond-charge repulsion and hole superconductivity, *Physica C: Supercond. Appl.* **158**, 326 (1989).
- ³⁷ J.E. Hirsch and F. Marsiglio, Hole superconductivity: Review and some new results, *Physica C: Supercond. Appl.* **62-164**, 591 (1989).
- ³⁸ L. Arrachea and A. A. Aligia, Pairing correlations in a generalized Hubbard model for the cuprates, *Phys. Rev. B* **61**, 9686 (2000).
- ³⁹ S. Jiang, D. J. Scalapino, and S. R. White, A single-band model with enhanced pairing from DMRG-based downfolding of the three-band Hubbard model, arXiv:2303.00756